Check for updates

Thermal dissipation as both the strength and weakness of matter. A material failure prediction by monitoring creep†

Tom Vincent-Dospital, [ID] *[ab] Renaud Toussaint, [ID] *[ab] Alain Cochard, [ID] [a] Eirik G. Flekkøy [ID] [b] and Knut Jørgen Måløy [ID] [b]

In any domain involving some stressed solids, that is, from seismology to general engineering, the strength of matter is a paramount feature to understand. We here discuss the ability of a simple thermally activated sub-critical model, which includes the auto-induced thermal evolution of cracks tips, to predict the catastrophic failure of a vast range of materials. It is in particular shown that the intrinsic surface energy barrier, for breaking the atomic bonds of many solids, can be easily deduced from the slow creeping dynamics of a crack. This intrinsic barrier is however higher than the macroscopic load threshold at which brittle matter brutally fails, possibly as a result of thermal activation and of a thermal weakening mechanism. We propose a novel method to compute this macroscopic energy release rate of rupture, G_a, solely from monitoring slow creep, and we show that this reproduces the experimental values within 50% accuracy over twenty different materials, and over more than four decades of fracture energy.

1 Introduction: from slow creep to abrupt rupture

Although seminal, the early theoretical descriptions of crack dynamics, such as Griffith's[2] or Slepyan's,[3,4] were somewhat binary: beyond a critical mechanical load, matter suddenly breaks. It is however acknowledged that, at load levels below the critical one, a far slower crack propagation already occurs, that will here be referred to as 'creep'. This phenomenon was successfully modelled with Arrhenius-like sub-critical growth laws,[1,5] and is hence sometimes called 'stress corrosion'. With the increasing number of experimental work, the description of such a slow dynamics was quickly refined, and five propagation stages were notably distinguished.[1] Let us start this manuscript by summarising them. Fig. 1 illustrates these stages in a V–G plot, where V is the crack velocity for a given load G, which is the 'energy release rate', that is, the energy that the fracture consumes to advance by unit surface.[2] At stage 0, while under only a mild mechanical input, cracks do not actually propagate forward. This was notably explained by the existence of some

healing processes, that there efficiently compete with the failure ones.[5] From this state, when the load is increased above a given threshold, some slow fracture growth starts to be observed (stage I). The propagation velocity V increases exponentially with the crack's energy release rate G. In a sub-critical (*i.e.*, Arrhenius-like) description, it implies that V is to first order explained by an activation mechanism dependent on G, in a chemical-like rupture reaction.[6] Logically, this regime was observed to also depend on the surrounding temperature and on the fluid which is present in the fracture,[7] which affects the chemical reaction involved in molecular bond breaking. When reaching a faster propagation, some velocity plateau might then hold (stage II), possibly as the transport of fluid corrosive elements toward the tip cannot efficiently cope with the crack advance. Such plateau is, in this case, only a transition to a sub-critical growth 'in-vacuum-condition', where the dynamics becomes notably insensitive to the fracture fluid (stage III). Finally, when a particular threshold is reached for the energy release rate, the velocity jumps to a far quicker regime: the material fails (stage IV). We will denote‡ this threshold G_a in J m^{-2}, with 'a' standing for 'avalanche'.

[a] *Université de Strasbourg, CNRS, ITES UMR 7063, Strasbourg F-67084, France.*
  E-mail: renaud.toussaint@unistra.fr
[b] *SFF Porelab, The Njord Centre, Department of Physics, University of Oslo,*
  N-0316 Oslo, Norway. E-mail: tom.vincent-dospital@fys.uio.no
† Electronic supplementary information (ESI) available: Derivation of eqn (7), sensitivity of the ϕ parameter, creep data for the presented materials, inverted parameters summary. See DOI: 10.1039/d0sm02089c

‡ This is usually referred to as G_c in experiments, since it corresponds to the value of the macroscopic energy release rate at which the velocity of fracture propagation jumps to much higher values. By contrast, in this article and our previous works, we made the choice to design as G_c a microscopic property, which corresponds to an actual energy barrier in the rupture process, and we consequently used a different notation, G_a, for the load at which cracks avalanche to a fast phase, as a result of a boosted thermal activation (*i.e.*, see Section 2). This notation choice is further discussed in Section 3.

In this work, we will show how studying the slow creep regime allows to predict this particular failure load. This can lead to methods to characterise natural or lowly controlled materials, where the critical energy release rate G_a is not well known a priori, but where the monitoring of creep allows to infer it. In a previous study,[8] we indeed proposed a unifying model of the slow creep and the fast regime, holding a precise quantification of the energy budget and the heating of the crack tip, which is coupled with an Arrhenius-type activation law. We have shown how it accounts, in some polymers,[9] for seven decades of propagation velocities and for the transition, at the avalanche load, from creep to sudden failure. Here, we present how well this thermodynamics based model can predict the threshold G_a for a broad range of materials, by comparing its forecasts to actual experimental failure thresholds from twenty data sets from the literature. By doing so, one can actually identify the microscopic rupture energy of the breaking bonds, G_c, and show how this quantity is related to, yet different from, the macroscopic G_a. The agreement between the predictions and the realisation is obtained for materials spanning more than 4 orders of magnitude in energy release rate, indicating the robustness of this description among different types of materials and the versatility of the theoretical framework.

2 The thermal weakening model

We consider that the propagation of a crack follows an Arrhenius sub-critical growth law, in which the temperature term accounts for the induced heat generated at the plastic crack tip.[10,11] Such a model, introduced in ref. 8 and 9, writes as

$$V = V_0 \min\left[\exp\left(-\frac{d_0^3(G_c - G)}{2lk_B(T_0 + \Delta T)}\right), \quad 1\right] \qquad (1)$$

$$\frac{\partial(\Delta T)}{\partial t} = \frac{\lambda}{C}\nabla^2(\Delta T) + \frac{\phi G V}{C\pi l^2}f, \qquad (2)$$

where the first equation describes the Arrhenius growth (i.e., the term in brackets is a probability for the thermal bath to overcome an energy barrier), and the second one in the diffusion equation governing the thermal evolution around the crack front. The heat conductivity and volumetric heat capacity of the solid matrix are respectively denoted λ and C. V_0 is a nominal atomic speed related to the collision frequency in the thermal bath, and should typically be comparable to the mechanical wave velocity of the studied media.[3,12] The activation energy is modelled proportional to $(G_c - G)$, where G_c is the surface energy barrier to overcome in order to break atomic bonds. d_0^3 is the characteristic volume for the bonds ($d_0 \sim 1$ Å), k_B is the Boltzmann constant, T_0 the ambient temperature and ΔT any variation away from it at the crack tip. A percentage ϕ of the power consumed per unit of crack length GV is uniformly dissipated as heat over a zone of support function f and of radius l. This heating zone is a subset of the process zone (that is, the full extent of plasticity around the tip), and we assume that it also constrains the stress level σ at the tip, as verified in Vincent-Dospital et al.:[9] $\sigma \sim \sqrt{GE/l}$ (e.g., see ref. 1), where E is the materials Young's modulus. This assumption is the

reason why l also intervenes in eqn (1), where the elastic energy stored in the rupturing link typically writes as $d_0^3\sigma^2/(2E)$, and is thus similar to $d_0^3G/(2l)$. In this framework, an acceleration of a fracture is thus both related to an increase of stress at the tip, which reduces the rupture energy barrier $d_0^3(G_c - G)/(2l)$, and to a related increase in volumetric internal energy ($C\Delta T$) at the fracture's head.

Note that it was shown[9,13] that, at low velocities (i.e., the creep velocities we are interested in), ΔT computed from eqn (2) can, more simply, be approximated to

$$\Delta T \sim \frac{(\phi G V h)(l/V)}{C(\pi\delta^2 h)} = \frac{\phi G V}{\lambda}, \qquad (3)$$

where ϕGVh is the thermal power deposited along a portion of length h of the crack front, l/V is the characteristic time for the front heating (i.e., the time a given location of the material stays in the advancing heating zone) and $\delta \sim \sqrt{\lambda l/(\pi CV)}$ is the skin depth of heat diffusion upon the same time. According to eqn (3), ΔT does not depend on C or l, notably because if the crack advances slowly enough, the temperature elevation is constrained by the heat diffusion skin depth δ rather than by the size of the heat production zone, as the former is, in this case, big compared to the latter.

Approximating eqn (1) and (2) by their steady state solutions, two stable propagation branches are derived from this model,[8] as shown in Fig. 2: a fast phase, which is obtained for a hot crack tip and corresponds to the catastrophic failure of matter, and a slow one corresponding to the creep regime, when $\Delta T \ll T_0$. In between these two branches, a hysteresis situation holds with a third unstable phase. In this study, we are mainly interested in the slow to fast regime transition (i.e., that leads to quick material failure).

When approaching this transition, the velocity deviates from its negligible heating asymptotic expression, which is a simple exponential increase with the load G:

$$\ln\left(\frac{V}{V_0}\right) \sim (G - G_c)\left[\frac{d_0^3}{2lk_BT_0}\right], \qquad (4)$$

as the rise in temperature ΔT in eqn (1) becomes comparable to the room temperature T_0. The particular energy release rate G_a is then reached, at which $\partial V/\partial G \to +\infty$, and beyond which the crack can only avalanche to a velocity which is orders of magnitude higher (see Fig. 2). Matter suddenly breaks. As a result of thermal activation, G_a is actually less than the actual surface energy barrier for breaking bonds G_c.

Although rarely regarded today, such an importance of the auto-induced heat to explain brittleness was early developed.[14–16] These studies reckon that the dissipated energy favours failure by locally softening the material at the tip (i.e., a decrease of its elastic moduli with temperature), in particular in the case of soft rubber-like materials. In the formalism of eqn (1), this view would correspond to a brutal reduction of the energy barrier $d_0^3(G_c - G)/(2l)$ at the onset of the instability, rather to (or maybe in addition to) a dramatic increase in temperature, due to chemicophysical phase changes of the matrix. Our model neglects such a softening effect and instead considers that the
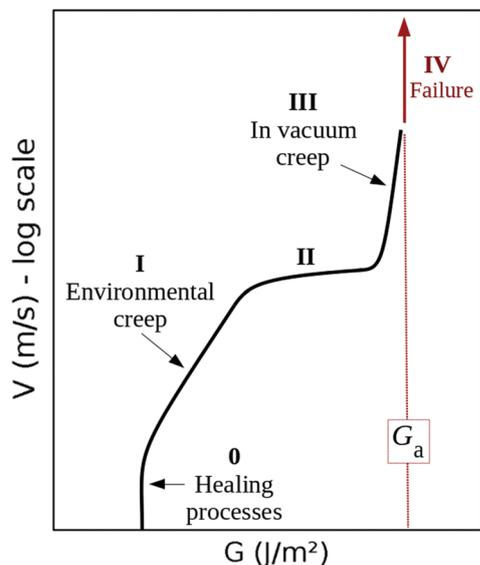
Fig. 1 Summary of the different forward crack velocity regions observed in experimental velocity curves. After Fracture of Brittle Solids, Lawn.[1]
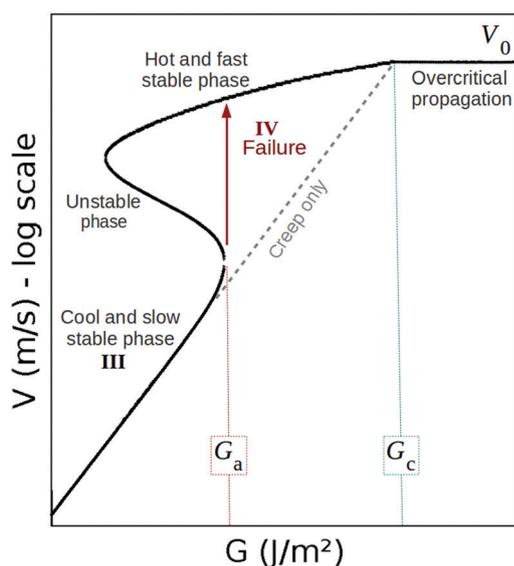

Fig. 2 Modelled crack velocity as a function of energy release rate, as per eqn (1) and (2). Stages III and IV correspond to those labelled in Fig. 1. As explained in the text, stages 0, I and II are here not covered. In our model, the failure occurs when the cracks becomes hot enough, that is, when $\Delta T \sim T_0$. The dashed line corresponds to a cold case $\Delta T \ll T_0$ in eqn (1).

reaction rate for rupture is increased from the elevated temperature, only as understood by statistical physics. Of course, both views are not mutually exclusive, and one of the two mechanisms may prevail depending on the considered material, or depending on the crack velocity. Indeed, for a softening effect to be at stake, the typical time for a material temperature-related change in phase must be less than the typical warming time l/V of a given location of the crack trajectory. By contrast, a change in velocity,

as understood by statistical physics, should be as quick as a few atomic vibrations[6] ($\sim 10^{13}$ Hz) and, hence, should be more likely to explain fast cracks in hard solids. Such a qualitative discussion underlines the importance of knowing the actual rheology close to crack tips in given materials, and its sensibility to eventual temperature bursts. Note that in both approaches of thermal weakening here discussed, the G value of interest (*i.e.*, G_a) remains similar in its concept: the threshold for which ΔT is high enough so that a quick avalanche can be generated by a given mechanism. In the rest of this manuscript, we will focus on the thermally activated, statistical, model that we have developed above, where the accurate rheology at the tip is actually considered to be of second order on the crack dynamics, and only the increase of ΔT is considered.

3 Model predictions *versus* reported failures

Extensive fracturing experiments on numerous materials can be found in the literature. Hence, we can compare the model predictions of G_a to some experimentally reported avalanche thresholds, that are often referred to as 'critical energy release rate' or 'material toughness', although it does not correspond to what is here denoted G_c, which is an intrinsic (microscopic) medium property not directly measurable at lab scale. In our framework, G_c is called the critical energy release rate because it differentiates between an actual subcritical propagation (at $G < G_c$), where thermal activation is required for the crack to advance, and an overcritical propagation (at $G > G_c$), where enough mechanical energy is given to the crack so that thermal activation is not strictly needed. In this latter case, eqn (1) simplifies to $V = V_0$. A fast 'dynamical' crack can be subcritical (see Fig. 2), in particular when $G_a < G < G_c$, and we thus refrained to call G_a a critical energy release rate.

Note that eqn (1) does not account for all of the creep regimes summarized in Fig. 1, that one can meet with an experimental test, but displays a unique low velocity slope (*i.e.*, from eqn (4)). We have indeed discarded any healing processes, needed to explain stage 0, as they are beyond the topic of the current study. Such processes can however be included in the model.[9] We have also assumed no rate-limiting environmental factor, that is, no significant chemical interaction of the matrix with the fracture fluid (*i.e.*, no stage I or II). We have hence restricted our comparison to experimental data to such a non-environmental creep case (stage III), although distinguishing it with certitude is not always straightforward. When available, we have notably preferred data sets of in-vacuum or dry (in air) experiments or with lowly corrosive (*e.g.*, neutral pH) fracture fluids (see the creep plots in the ESI† for an exhaustive list of the considered experiments, and their environmental conditions).

Indeed, high fluid pH or moisture tend to increase the creep dynamics of given materials (*e.g.*, ref. 17), presumably by altering the chemistry of the rupture process at the tip (*i.e.*, stages I and II), and such effects are not included in our model. Note however that, when some fluid–matrix interaction does take place, the model

could still be somewhat applied, if failure is preceded by a unique slope (*i.e.*, if it occurs before the slope break between stages I and II), or after it, once clearly having entered in regime III. In the former case, the definition of the surface energy barrier G_c may slightly change: from an intrinsic strength of the solid to an equivalent (lower) strength under a given chemical environment.

To predict G_a, it is of course needed to know, for each material, the values of the model constitutive parameters, that is, the parameters of eqn (1) and (2), which describe the evolution of the crack velocity as a function of the applied energy release rate. Although they are not many, most of these parameters are not usually considered, and are hence unknown. It is however possible to estimate their order of magnitude from known material properties, or to assess them from the slow (creep) part of the loading curve. We have first considered that V_0 is of the order the mechanical wave velocity. It could ideally be that of the Rayleigh waves,[12] but it is often simpler to instead estimate the – similar – shear wave velocity of solids, $V_S \sim \sqrt{\mu/\rho}$, as the shear modulus μ and the density ρ of most materials are easily available. The heat conductivity λ is also known in most cases, and T_0 is nothing but the room temperature at which a given reported experiment took place. We assume the inter-atomic space d_0 to be 1 Å. While it could be two or three times larger depending on the materials, which would have an order of magnitude effect on the term d_0^3, this uncertainty would only impact the estimation of l, as the ratio d_0^3/l is here of importance. We indeed have to deduce l and G_c from the slope and intercept of the slow sub-critical growth, that is, from the two terms of eqn (4) fitted to the experimental curves with the fit parameters V_{null} and b: $\ln(V/V_{null}) = bG$, V_{null} being the velocity a crack would have at a null load ($G = 0$), in the absence of fluid corrosion or healing effects and b the slope of the creep curve of dimension m³ s⁻¹ J⁻¹. This gives

$$l = \frac{d_0^3}{2bk_BT_0} \tag{5}$$

for the size of the thermal zone, and, for the intrinsic strength of the solid:

$$G_c = \frac{2lk_BT_0}{d_0^3}\left[\ln\left(\frac{V_0}{V_{null}}\right)\right]. \tag{6}$$

This implies that we can predict G_a if relying on some creep observations, that can yet be at loads far below the failure threshold. The only remaining model parameter, the percentage ϕ of energy converted into heat is mostly unknown. While qualitative statements, such as larger ϕ in metals rather than, say, polymers, are tempting, we have here arbitrarily fixed this percentage to 50% in all materials, except for a couple of instances where we could estimate it.[9,13] For different materials, we however show how ϕ affects the prediction of our model in the ESI.†

Note that, while the velocity is often reported in relation to the stress intensity factor K rather than the energy release rate G, we have here converted from one to the other with the following relation:[1] $G \sim K^2/E$ to derive a and b, and then l and G_c. Backwardly, with the here proposed method, we will thus

predict the toughness, $K_{avalanche} \sim \sqrt{EG_a}$, based on the creep measurement. All the introduced parameters can now be estimated, and we did so for twenty materials for which the creeping behaviour was studied in the literature.[9,17–34] The corresponding G to V curves and a table of all the inferred parameters values are shown in the ESI.† We can then solve numerically the two non linear eqn (1) and (2), now taking into account the temperature rise ΔT. In other words, for any value of the energy release rate G, we can compute the possible crack propagation velocities according to the model, as for instance shown in Fig. 2, where, depending on G, one to three velocities are possible. The inflection of the obtained curve, where $\partial V/\partial G \to +\infty$ (see Fig. 2), can be identified as G_a and compared to the reported experimental thresholds. The detailed procedure is discussed and applied to two materials (PMMA and Pressure Sensitive Adhesive) in ref. 9. This comparison is summarised for all the media in Fig. 3, and our model displays there a good general description of catastrophic failure. In the same figure, the surface energy barrier G_c is also displayed for comparison, as well as the relative error made in the estimation of G_a.

4 Analytical approximation

While, to derive the modelled G_a, one should compute the full crack dynamics (*i.e.*, as displayed in Fig. 2), and search for the points where $\partial G/\partial V = 0$, we explain in the ESI† how eqn (1) and (2) also approximately lead to

$$G_a \sim \frac{\lambda T_0}{\phi V_0}\frac{\exp(R_a)}{R_a}, \tag{7}$$

where R_a is the activation energy at the avalanche threshold counted in thermal energy units: $R_a = d_0^3(G_c - G_a)/(2lk_BT_0)$. As this ratio notably depends on G_a, eqn (7) only implicitly defines the threshold. Although a numerical solver is there still required to compute the threshold, it is simpler and far quicker than finding the accurate solution, and potentially easy to use in engineering applications.

We show, in the ESI,† how the approximation of eqn (7) is a slight overestimation of the real solution, by about 0 to 10%. It however gives further insight on the influence of each parameter. The remaining dependence on $(G_c - G_a)$ shows that, to obtain thermal weakening, one must already be close to the actual microscopic energy barrier of rupture G_c. The stress at the tip thus remains an important driving mechanism of the crack propagation. The brutal failure threshold G_a increases with the ambient temperature T_0, as a higher temperature elevation ΔT is then required at the tip to significantly overcome a higher thermal bath. Similarly, G_a increases with the λ/ϕ ratio, as a high λ/ϕ indicates a rather cool crack tip, either because little energy is converted into heat (*i.e.*, a small ϕ) or because this energy is efficiently evacuated away from the crack (*i.e.*, a high λ). The failure threshold also decreases with V_0, as, at a given load, a higher V_0 means a faster (and then hotter) creeping crack from a higher atomic collision frequency V_0/d_0.

5 Microscopic *vs.* macroscopic fracture energy, and local *vs.* bulk energy dissipation

In Fig. 3, one can notice that the surface energy barrier G_c is always similar in order of magnitude to the rupture threshold G_a. Yet, the rupture always occurs at a load less than G_c, with G_a being about twice lower in average for all the displayed solids. We have here explained how a weakening mechanism, as the thermal view that we have here developed, allows to account for this discrepancy.

Having gathered various exponential creep data, and derived l and G_c from their slope and intercept in their $\ln V - G$ representations, we can notably infer the intrinsic crack energy barrier in each material: $U_c = d_0^3 G_c/(2l) = k_B T_0 \ln(V_0/V_{null})$. As shown in Fig. 4, this quantity is always in the order of 10^{-19} J–1 eV, logically comparable to the energy level necessary to unbind single atomic covalent bounds,[35] which confirms the relevance of a simple thermally activated model for the description of stage III (in-vacuum-like) creep. The actual values of U_c are yet often slightly smaller than the typical covalent strength. This could derive from an averaging effect. Indeed, the Arrhenius law of eqn (1) is a mesoscopic statistical law, which we have fitted to some macroscopic measurements of crack propagation (*i.e.*, the creep experiments). With cracks that are prone to follow the weakest paths, that possibly include weak inter-molecular bonds (such as van der Waals and hydrogen links) and dislocations or atomic voids (*i.e.*, when the distance between two consecutive breaking bonds is more than a few Ångströms),
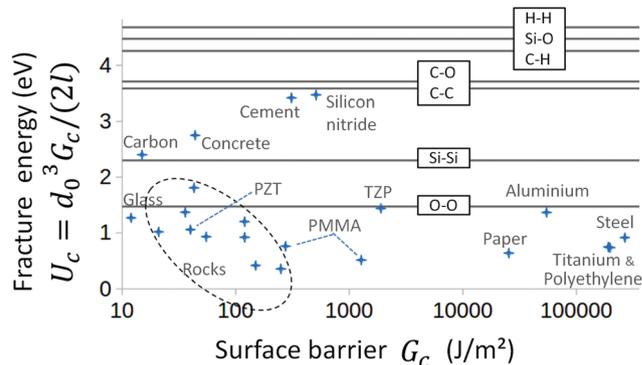

Fig. 4 Microscopic fracture energy $U_c = d_0^3 G_c/(2l)$ as a function of the macroscopic energy barrier G_c, for the same materials as in Fig. 3. See the ESI† for the exhaustive list. Note that the accuracy of U_c is not better than an order of magnitude. The horizontal lines show some typical covalent cohesion energies for comparison.[35]

U_c is likely representative of the average rupture energy in a disordered landscape. For instance, in polymers, part of the rupture shall be inter-molecular, and, in rock-type materials, the crack dynamics might benefit from the intrinsic porosity. However, due to the simplicity of the model, care should be taken when interpreting U_c beyond its order of magnitude.

It is clear however that the value of G_c varies by a factor 10^4 for different materials, while its counterpart U_c does not. As most materials have the same U_c and d_0, in order of magnitude, the large variability in G_c (and hence in G_a) which is observed is, in this description, attributable entirely to the variability in the
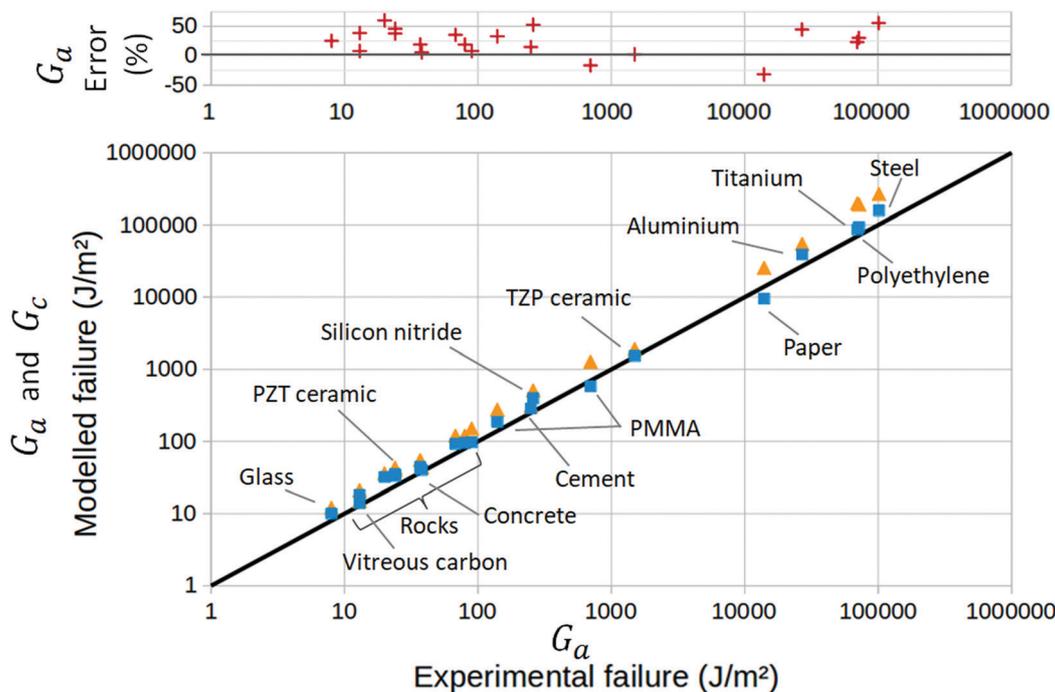

Fig. 3 (bottom) Modelled G_a thresholds (squares) and modelled surface energy barrier G_c (triangles) compared to the experimental thresholds from the literature. The black line is the identity. The labels locate different materials. The unlabelled rock materials are quartz, sapphire, granite and andesite. See the ESI† for an exhaustive list. (top) Relative error on the avalanche threshold.
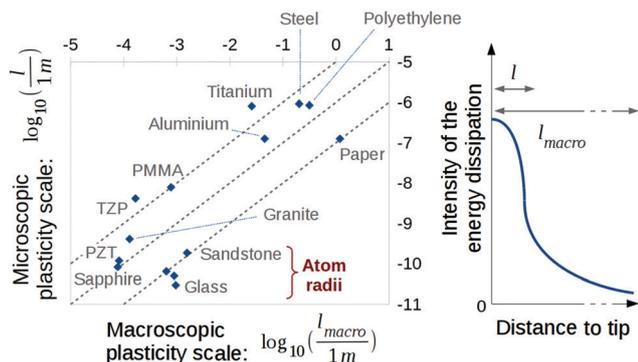
Fig. 5   (left) Core size of the process zone l, as understood by our model, *versus* macroscopic plasticity scale l_{macro}, as derived from reported tensile yield stresses. The straight lines mark a factor 10^5, 10^6 and 10^7 between both views. The two unlabelled points in the vicinity of glass represent quartz and concrete. (right) Simplified spacial distribution of the intensity (arbitrary unit) at which energy is dissipated (*i.e.*, plasticity) around the crack tip, as a possible explanation for the difference in scale. The graph is not to scale, as $l_{macro} \gg l$.

scale for the release of heat. We indeed infer that l varies from the radius of a single atom, for the weakest materials, up to 1 μm, for the ones with the highest G_c (see Fig. 5). The wider the plastic area that shields crack tips, the stronger matter is. But backwardly, we have discussed how the heat dissipation might be the root cause for dramatic ruptures in brittle solids, if the heat is not efficiently evacuated away from the rupture front. Overall, eqn (1) should be understood as:

$$V = V_0 \exp\left(-\frac{U_c - U(\text{Load}^{[+]}, \text{ Thermal radius}^{[-]})}{k_B T(\text{Thermal dissipation}^{[+]}, \text{ Diffusion}^{[-]})}\right),$$
(8)

where U is the mechanical energy corresponding to the stress actually transmitted to the crack tip covalent bond of average strength U_c, and where [+] and [−] indicate whether the T and U functions are increasing or decreasing with the specified concepts (*i.e.*, with the mechanical load, the core (thermal) dissipation radius l, the dissipation of heat or its diffusion). This equation emphasises that, in our formalism, thermal dissipation is both the strength of matter (from the shielding of the mechanical energy U actually transmitted to the crack tip) and the weakness of matter (from the amplification in internal energy around the tip).

We can compare the values of l with the more typical plastic radius predicted by a Dugdale view[36] of the process zone, $l_{macro} \sim G_c E/\sigma_y^2$, where σ_y is the tensile yield stress, beyond which macroscopic samples lose their elasticity. As shown in Fig. 5, the latter is consistently five to seven orders of magnitude higher than what we predict for l. This likely translates to the fact that plasticity (here understood as the dissipation of mechanical energy in any form) ought to be a rather heterogeneous phenomenon, with a greater density of energy dissipation close to the front than away from it. A higher density of energy is indeed likely to be dissipated close to the tip singularity than at the edge of the l_{macro} plastic radius. Thus, the scale of a process zone can be characterised either by its core radius l, where

most of the heating due to the dissipation takes place, or by its full extent l_{macro}, where the rheology becomes non elastic. While the former is to include significant thermal losses (quantified by ϕG), the latter can also encompass various other dissipation mechanisms for another portion of G, namely, the nucleation of dislocations, the release of extra heat over a greater volume around the tip, the emission of phonons and photons, or even some material change in phase (*e.g.*, softening). In our formalism, l is also the main parameter that describes the shielding of the stress near the crack tip, and this stress is indeed likely to be higher at the centre of the process zone than at its periphery, calling for $l < l_{macro}$. Large scale bulk energy losses (*e.g.*, ref. 37 and 38) are hence permitted by our model, and we only state that it is of second order effect on the temperature elevation and the stress level at the crack front and, hence, on the crack dynamics.

Besides its straight derivation from a canonical kinetics law (*i.e.*, eqn (1)), there are various indicators suggesting that, although smaller than the more common l_{macro}, the sizes l that we have inverted bear a strong physical significance. For materials where l is here computed to be relatively large (*i.e.*, in the micrometer range) infrared emissions can easily be recorded around (hot) crack tips by standard resolution infrared cameras, such as in paper[13] or steel.[39] In the case of paper, we inferred l close to the micrometric domain, which is about the dimension of the fibril forming this media. For running cracks in materials with a smaller l, such as PMMA or even glass, a hot temperature could also be derived by the characterisation of light emission,[40,41] although its observation is not as straightforward. In glass,[41] in particular, the light emission lies in the visible domain, calling for blackbody[42] temperatures elevations of thousands of kelvins, and the light emitting zone was shown to have a nanometric radius. In PMMA, secondary microcracks tend to nucleate ahead of fast fronts from cavities/bubbles of about 100 nm in radius,[9] possibly initiated by sublimation at hot temperature of the solid matrix. In rocky materials, nanometric damages can be observed[43] on fault planes. These planes are sometimes referred to as fault mirrors, due to their glossy appearance arising from their very low roughness at the visible light wavelengths. Intense thermal effects, often referred to as 'flash heating', are notably suspected for the instability of some seismic faults.[44,45]

Overall, some intense, extremely localised (*i.e.*, l), dissipation processes close to rupture fronts are thus likely to explain these various observations, and, in our framework, could also explain the brittleness of matter.

6 Discussion and conclusion

We have thus presented a model that gives reasonable predictions of the rupture load, over a broad range of materials. We did this with a full expression (eqn (1) and (2)), or in simplified forms (eqn (1) and (3) or eqn (7)). This predicted load is still, however, overestimated by about 25% (in average for all media, see the errors in Fig. 3). This could derive from numerous causes. First, most of our parameters were only broadly estimated, when not

arbitrarily fixed. We have in particular assumed that G_c is a homogeneously distributed constant, whereas it is likely to hold some level of quenched disorder.[46,47] In this case, the overall creep dynamics (*i.e.* the slow branch of Fig. 2, described by eqn (4)) would not be strongly affected, as it shall mainly depend on an average value of G_c. The failure, however, would be prone to occur on weaker locations,[8] that are controlled by a lower G_c, which would explain our overestimation of G_a. It corresponds to the common idea that the overall strength of a material is highly dependent on its heterogeneities. As discussed in Section 5, our computation of the microscopic energy barrier U_c likely represents the average of a disordered landscape in dissociation energy, as its value lies in between that of an actual covalence energy and those of weaker interactions. Additionally, we derived G_c from the mean fit to experimental creep curves that, in some materials, hold some significant data dispersion (see the ESI†). Some of this dispersion could arise from mesoscopic fluctuations of macroscopic fracture energy G_c in these materials, and the avalanche threshold G_a could be highly dependent on the standard deviation of these fluctuations. Another explanation for the overestimation of G_a could be that the experimental error on the measurement of this parameter may in practice be important, as the avalanches occur in a regime where the crack velocity diverges with G, just before test samples snap at a velocity comparable to that of the mechanical waves. Hence, the last mechanical load accurately measured before rupture is, by essence, to be slightly below the actual physical threshold. Note also that, sometimes, the actual creep stage (*i.e.*, 0 to III in Fig. 1) that we fit to derive our parameters is not unambiguously identifiable on the experimental curves, while our theory does not encompass fluid-to-matrix interactions. Besides these considerations, the model is extremely simple, applying mesoscopic laws (*i.e.*, Fourier conductivity and Arrhenius growth) at atomic scales. For instance, a propagative description[48] of the heat transport (*i.e.*, not assuming, such as Fourier diffusion, an infinite transport velocity) could be needed, due to the small time and space scales that are here considered. Overall, a transposition of the model into a, more complicated, atomistic solver[49] would be beneficial.

Of course, the fact that the model reproduces an instability does not necessarily mean that it is the only explanation for britleness. Other models (*e.g.*, the thermal softening of the matrix around the tip,[16] or the perturbation of the stress field ahead of the crack by the rupture-induced emission of high frequency phonons[3]) have been proposed for this instability, and, in practice, depending on the materials, more than one physical process could here be at stake. Still, the model we propose gave, in some instances,[9] a comprehensive explanation of the full dynamics of failure. Additionally, we have here shown how G_c, the intrinsic surface energy barrier of materials, shall only depend on a heat dissipation scale around the crack tip, and that the accumulation of this induced heat is effectively reducing the mechanical resistance of matter ($G_a < G_c$).

Countering this latter effect could be a key to design advanced strong materials, in particular as some intriguingly tough solids such as graphene[50,51] or arachnid silks[52] are indeed very conductive. Interestingly, the conductivity of spider threads even increases with deformation,[52] which could be a nature made adaptive defence mechanism for the stability of nets, whenever they are pressurized. Replicating such a behaviour with a man-made material would then be an important achievement that could lead to high performance cables or bulk materials. For instance, a first step could be the engineering of highly conductive atomic networks, integrated into strong solid matrices, thus limiting any local rise in temperature that could weaken matter. A more down-to-earth application of the model could be the monitoring of structures and infrastructures, as we have shown how their creep rate can be used to predict their failure. This would be of particular interest for bodies that have aged in uncontrolled conditions, in which the change in mechanical properties becomes uncertain with time, but could be inverted from their creep.

Finally, and although we have only treated about fracture in mode I, we suggest that most of the effects that we have discussed shall be valid for mixed-mode fracturing and solid friction. The latter is also suspected to hold some non negligible, thermal related, weakening mechanisms,[44,45] which could notably be a key in geophysics and in understanding the stability of seismic faults. In particular, when increasing the background temperature T_0, it was shown that the model holds a critical point, beyond which not enough heat can be generated to trigger instabilities in the dynamics of cracks,[8] which may physically explain the brittle-ductile transition in the Earth's crust,[53,54] below which rocks tend to flow rather than break.

Conflicts of interest

There are no conflicts to declare.

Acknowledgements

References

1 B. Lawn, *Fracture of Brittle Solids*, Cambridge University Press, 2nd edn, 1993.
2 A. Griffith, *Philos. Trans. R. Soc. London, Ser. A*, 1921, **221**, 163–198.
3 L. Slepyan, *Sov. Phys., Dokl.*, 1981, **26**, 538–540.
4 M. Marder, *Philos. Trans. R. Soc., A*, 2019, 20190098.
5 J. Rice, *J. Mech. Phys. Solids*, 1978, **26**, 61–78.
6 G. G. Hammes, *Principles of Chemical Kinetics*, Academic Press, 1978.
7 N. Brantut, M. J. Heap, P. G. Meredith and P. Baud, *J. Struct. Geol.*, 2013, **52**, 17–43.

8 T. Vincent-Dospital, R. Toussaint, A. Cochard, K. J. Måløy and E. G. Flekkøy, *Phys. Rev. Mater.*, 2020, 023604.

9 T. Vincent-Dospital, R. Toussaint, S. Santucci, L. Vanel, D. Bonamy, L. Hattali, A. Cochard, K. J. Måløy and E. G. Flekkøy, *Soft Matter*, 2020, 9590–9602.

10 E. Orowan, *Energy criteria of fracture*, Massachusetts institute of technology, cambridge departement of mechanical engineering technical report, 1954.

11 G. R. Irwin, *J. Appl. Mech.*, 1957, **24**, 361–364.

12 L. B. Freund, *J. Mech. Phys. Solids*, 1972, **20**, 129–152.

13 R. Toussaint, O. Lengliné, S. Santucci, T. Vincent-Dospital, M. Naert-Guillot and K. J. Måløy, *Soft Matter*, 2016, **12**, 5563–5571.

14 G. P. Marshall, L. H. Coutts and J. G. Williams, *J. Mater. Sci.*, 1974, **9**, 1409–1419.

15 D. Maugis, *J. Mater. Sci.*, 1985, **20**, 3041–3073.

16 G. Carbone and B. N. J. Persson, *Phys. Rev. Lett.*, 2005, **95**, 114301.

17 P. M. Dove, *J. Geophys. Res.: Solid Earth*, 1995, **100**, 22349–22359.

18 O. Lengliné, R. Toussaint, J. Schmittbuhl, J. E. Elkhoury, J. P. Ampuero, K. T. Tallakstad, S. Santucci and K. J. Måløy, *Phys. Rev. E: Stat., Nonlinear, Soft Matter Phys.*, 2011, **84**, 036104.

19 S. Santucci, PhD thesis, Ecole Normale Supérieure de Lyon, 2004, www.theses.fr/2004ENSL0288.

20 M. Yoda, M. Nabetani and W. Shim, *Int. J. Fract.*, 2001, **112**, 21–26.

21 S. M. Wiederhorn, *J. Am. Ceram. Soc.*, 1967, **50**, 407–414.

22 S. Wiederhorn and R. J. Krause, *Ceramic Engineering and Science Proceedings*, 2002, pp. 71–82.

23 P. Meredith and B. Atkinson, *Phys. Earth Planet. Inter.*, 1985, **39**, 33–51.

24 Y. Nara and K. Kaneko, *Int. J. Rock Mech. Min. Sci.*, 2005, **42**, 521–530.

25 J. Holder, J. E. Olson and Z. Philip, *Geophys. Res. Lett.*, 2001, **28**, 599–602.

26 W. Wang, T. Tong and Q. Yu, 9th International Conference on Fracture Mechanics of Concrete and Concrete Structures, 2016.

27 Y. Nara, M. Takada, D. Mori, H. Owada, T. Yoneda and K. Kaneko, *Int. J. Fract.*, 2010, **164**, 57–71.

28 W. S. Oates, C. S. Lynch, D. C. Lupascu, A. B. K. Njiwa, E. Aulbach and J. Rödel, *J. Am. Ceram. Soc.*, 2004, **87**, 1362–1364.

29 J. Chevalier, C. Olagnon and G. Fantozzi, *J. Am. Ceram. Soc.*, 1999, **82**, 3129–3138.

30 A. G. Evans and S. M. Wiederhorn, *J. Mater. Sci.*, 1974, **9**, 270–278.

31 G. Hénaff, G. Odemer and B. Journet, *Aluminium Alloys, Theory and Applications*, IntechOpen, 2011, pp. 259–282.

32 J. H. Huang and C. J. Altstetter, *Metall. Trans. A*, 1991, **22**, 2605–2618.

33 S. M. L. Sastry, R. J. Lederich and B. B. Rath, *Metall. Trans. A*, 1981, **12**, 83–94.

34 J. S. Nadeau, *J. Am. Ceram. Soc.*, 1974, **57**, 303–306.

35 G. B. Kaufman, *J. Chem. Educ.*, 1993, **70**, A279.

36 D. Dugdale, *J. Mech. Phys. Solids*, 1960, **8**, 100–104.

37 J. Slootman, V. Waltz, C. J. Yeh, C. Baumann, R. Göstl, J. Comtet and C. Creton, *Phys. Rev. X*, 2020, **10**, 041045.

38 J. Samaca Martinez, E. Toussaint, X. Balandraud, J.-B. Le Cam and D. Berghezan, *Mech. Mater.*, 2015, **81**, 62–71.

39 D. Palumbo, R. De Finis, F. Ancona and U. Galietti, *Eng. Fract. Mech.*, 2017, **181**, 65–76.

40 K. N. G. Fuller, P. G. Fox and J. E. Field, *Proc. R. Soc. London, Ser. A*, 1975, **341**, 537–557.

41 G. Pallares, C. L. Rountree, L. Douillard, F. Charra and E. Bouchaud, *Europhys. Lett.*, 2012, **99**, 28003.

42 P. Jain and L. Sharma, *J. Appl. Sci. South Afr.*, 1998, **4**, 80–101.

43 S. Siman-Tov, E. Aharonov, A. Sagy and S. Emmanuel, *Geology*, 2013, **41**, 703–706.

44 J. R. Rice, *J. Geophys. Res.: Solid Earth*, 2006, **111**, B05311.

45 G. A. Prieto, M. Florez, S. A. Barrett, G. C. Beroza, P. Pedraza, J. F. Blanco and E. Poveda, *Geophys. Res. Lett.*, 2013, **40**, 6064–6068.

46 K. T. Tallakstad, R. Toussaint, S. Santucci, J. Schmittbuhl and K. J. Måløy, *Phys. Rev. E: Stat., Nonlinear, Soft Matter Phys.*, 2011, **83**, 046108.

47 A. Cochard, O. Lengliné, K. J. Måløy and R. Toussaint, *Philos. Trans. R. Soc., A*, 2018, 20170399.

48 D. W. Tang and N. Araki, *Int. J. Thermophys.*, 1997, **18**, 493.

49 C. L. Rountree, R. K. Kalia, E. Lidorikis, A. Nakano, L. Van Brutzel and P. Vashishta, *Annu. Rev. Mater. Res.*, 2002, **32**, 377–400.

50 Y. Hwangbo, C.-K. Lee, S.-M. Kim, J.-H. Kim, K.-S. Kim, B. Jang, H.-J. Lee, S.-K. Lee, S. Kim, J.-H. Ahn and S.-M. Lee, *Sci. Rep.*, 2014, **4**, 4439.

51 A. Balandin, S. Ghosh, W. Bao, I. Calizo, D. Teweldebrhan, F. Miao and J. Lau, *Nano Lett.*, 2008, **8**, 902–907.

52 X. Huang, G. Liu and X. Wang, *Adv. Mater.*, 2012, **24**, 1482–1486.

53 C. H. Scholz, *Geol. Rundsch.*, 1988, **77**, 319–328.

54 E. Aharonov and C. H. Scholz, *J. Geophys. Res.: Solid Earth*, 2019, **124**, 2721–2737.